New Journal of Physics
The open access journal at the forefront of physics

Deutsche Physikalische Gesellschaft DPG
IOP Institute of Physics

Published in partnership with: Deutsche Physikalische Gesellschaft and the Institute of Physics

OPEN ACCESS

RECEIVED
9 January 2017

REVISED
3 March 2017

ACCEPTED FOR PUBLICATION
24 March 2017

PUBLISHED
11 April 2017

Original content from this work may be used under the terms of the Creative Commons Attribution 3.0 licence.

Any further distribution of this work must maintain attribution to the author(s) and the title of the work, journal citation and DOI.

PAPER

Polaronic quantum diffusion in dynamic localization regime

Yao Yao

Department of Physics, South China University of Technology, Guangzhou 510640, People's Republic of China

E-mail: yaoyao2016@scut.edu.cn

Keywords: quantum diffusion, dynamic localization, organic materials

Abstract

We investigate the quantum dynamics in a disordered electronic lattice by the time-dependent density matrix renormalization group algorithm. The on-site energy in the lattice follows the Fibonacci sequence and the electron off-diagonally couples to a sub-Ohmic phonon bath. It is found that the slope of the inverse participation ratio versus the coupling strength undergoes a sudden change that indicates a transition from static to dynamic localization, and that the generated polarons coherently diffuse via hopping-like processes, evidenced by the saturated entanglement entropy, providing a novel scenario for a transportation mechanism in strongly disordered systems. Moreover, the mean-square displacement is revealed to be insensitive to the coupling strength, implying the quantum diffusion behavior survives the energy disorder that prevails in real organic materials.

1. Introduction

In the theory of localization phenomena in electronic systems [1], it is observed that the wavepacket of an electron cannot transport out of the regime scaled by the localization length in disordered systems [2]. This poses a big challenge to reveal the transportation mechanism of both excitons and charge carriers in organic molecules [3]. As an important alternative to silicon-based semiconducting materials, organic molecules suffer from a strong disorder even in their crystalline phase, which is thought to originate from thermally induced intermolecular phonon vibrations [4], and incoherent hopping between molecules was thus regarded as inevitable [5]. Recent advances in experiments on organic photocells, however, suggest the essential role played by the delocalization in the ultrafast charge separation process [6], in which an electronic band with delocalized wavefunction serves as a transport channel for the photogenerated charges [7]. Meanwhile, the ubiquitous electron-phonon (e–p) interactions were thought to play a unique and critical role in suppressing the influence of disorder and on the formation of the transport band, as indicated both experimentally and theoretically [8–11]. These two contrary perspectives of e–p interaction subsequently turn out to be a perfect starting point for clarifying the crossover between the diffusion and delocalization mechanisms.

When it comes to the physical origin of localization, Anderson proposed that lattice deformation may break translational invariance and open a large mobility gap in the band [2]. Investigations into the two issues of disorders and phonons have since advanced independently of each other. In organic systems, for e.g., disorders were studied mainly by kinetic Monte Carlo simulations [12] and phonons were investigated within the framework of small-polaron transformation [13]. The situation changed after Troisi *et al* proposed the concepts of dynamic-disorder and dynamic localization in 2006 [14] and 2010 [15] respectively, which established a possible connection between disorder and phonons. Since this, a great deal of research has been undertaken to comprehend the charge transport mechanism in organic crystalline materials by taking both issues into consideration [16–19]. Based on the Ehrenfest dynamics, we also proposed a mechanism that can combine the bandlike and hopping transports by introducing decoherence time into the electron dynamics [17].

More recently, Di Sante *et al* unravelled a novel metal-insulator phase transition considering both the disorder and the e–p interaction in organic molecules [20, 21]. They found that in the weak-interaction limit of a strongly disordered system, a mobility gap is opened at the Fermi energy along with the disappearance of the gap of density-of-states. In a sense, this implies that the formed polaron is mobile, making the strongly disordered

© 2017 IOP Publishing Ltd and Deutsche Physikalische Gesellschaft

system poorly conducting. The parameters characterizing the poor conductor phase are of broad relevance especially to organic materials, offering an alternative explanation of the charge transport in terms of the quantum diffusion of polarons. In order to see how the polaron moves in the disordered system with the assistance of phonons, in this paper we present a full quantum dynamical study of polaron diffusion in the so-called Fibonacci lattice. The dynamic localization picture will be re-examined in a dynamical manner to discuss its applicability in elucidating the mechanism of charge generation in organic solar cells. The paper is organized as follows. In section 2 the Hamiltonian model and the numerical method are described. The main results are presented in section 3 and a brief summary is presented in the final section.

2. Model and methodology

We first define a one-dimensional tight-binding Hamiltonian as ($\hbar = 1$)

$$H = \sum_i \epsilon_i c_i^\dagger c_i + \sum_\mu \left[\omega_\mu \hat{b}_\mu^\dagger \hat{b}_\mu + \gamma_\mu (\hat{b}_\mu^\dagger + \hat{b}_\mu) \cdot \sum_i (c_i^\dagger c_{i+1} + \text{h.c.}) \right], \tag{1}$$

where $c_i^\dagger$ (c_i) creates (annihilates) an electron at the i-th site, with the on-site energy ϵ_i; $\hat{b}_\mu^\dagger$ ($\hat{b}_\mu$) is the creation (annihilation) operator of the phonons, with the frequency being ω_μ, and γ_μ is the off-diagonal e–p coupling strength. Herein the model consists of two terms, the on-site energy of electrons with certain degrees of disorder, and the phonons off-diagonally coupling to the electron which acts as an equivalent hopping term to that in the normal tight-binding model. It is worth noting that the electronic coupling between nearest sites is set to be zero, since in organic materials the charge carrier is always localized in few molecules showing strong static disorder.

In order to get rid of the numerical uncertainty in generating random on-site energy, a Fibonacci sequence is assigned to ϵ_i, which is generated as follows [22, 23]. An energy scale ϵ_0 is firstly defined so as to characterize the degree of disorder, and then the sequences of on-site energy are generated by the recursion formula

$$L_1 = \{-\epsilon_0\},\ L_2 = \{\epsilon_0\},\ L_{i+1} = \{L_i, L_{i-1}\}\ (i \geqslant 2). \tag{2}$$

With this procedure of generation we obtain a series of lattices with quasi-disordered permutations of on-site energy, namely $L_3 = \{\epsilon_0, -\epsilon_0\}$, $L_4 = \{\epsilon_0, -\epsilon_0, \epsilon_0\}$, $L_5 = \{\epsilon_0, -\epsilon_0, \epsilon_0, \epsilon_0, -\epsilon_0\}$, ···. The number of the lattice site is given by the Fibonacci number, defined as $F_{i+1} = F_i + F_{i-1}$, with $F_1 = F_2 = 1$. It is well-known that in a Fibonacci lattice an electron exhibits super-diffusion around the original site, with the mean-square displacement (MSD) being proportional to $t^{1.55}$ and t being the time [23]. An electric field will give rise to localization, with the localization length depending on both the energy disorder and the field [22]. We do not intend in this work to consider the electric field but merely to focus on the e–p coupling, which will also induce dynamic localization, as discussed later. It is also worth noting here that the utilization of the Fibonacci sequence is mainly aimed at avoiding statistical averaging and to reduce the computational cost. The different generating method of the disordered site energy would give rise to slightly different results in a quantitative way, as shown in the following, while the qualitative conclusion drawn in this paper is robust and generic.

Instead of dealing with a single phonon mode [10], we hereby study a phonon bath coupled to the electrons, with the spectral density being continuous as $J(\omega) = 2\pi\alpha\omega_c^{1-s}\omega^s e^{-\omega/\omega_c}$. We have three parameters in the spectral function, namely the cut-off frequency ω_c, the exponent s, and the dimensionless coupling α. In practice, ω_c is taken to be 2.0, sufficiently large to eliminate any influence on the results. s and α together determine the e–p coupling strength. $s < 1$ denotes the sub-Ohmic phonon bath, which gives rise to a strong non-Markovian effect benefiting the dynamic localization effect, as discussed later. For simplicity, we fix s to be 0.5, a moderate value for organic materials [11, 29]. Subsequently, we have two free parameters in total in the system, i.e., ϵ_0 denoting the degree of the disorder and α denoting the e–p coupling strength. It obviously does not matter to fix ϵ_0 to be 0.1 as the energy unit and to merely adjust α in the computations.

The orthogonal polynomials adapted time-dependent density matrix renormalization group algorithm [24–30] is employed to calculate the dynamics of Hamiltonian (1). Initially the population of the electron is set to localize on the center of the lattice and the phonons are at the ground state. We do not consider the finite temperature effect for the phonons, and it can be expected that at finite temperature the coherence should be more easily lost so that the exponent for the super-diffusion behavior discussed later will be closer to 1. Throughout the work, the total number of sites is 34 (the ninth Fibonacci number), being sufficiently large to eliminate the finite size effect.

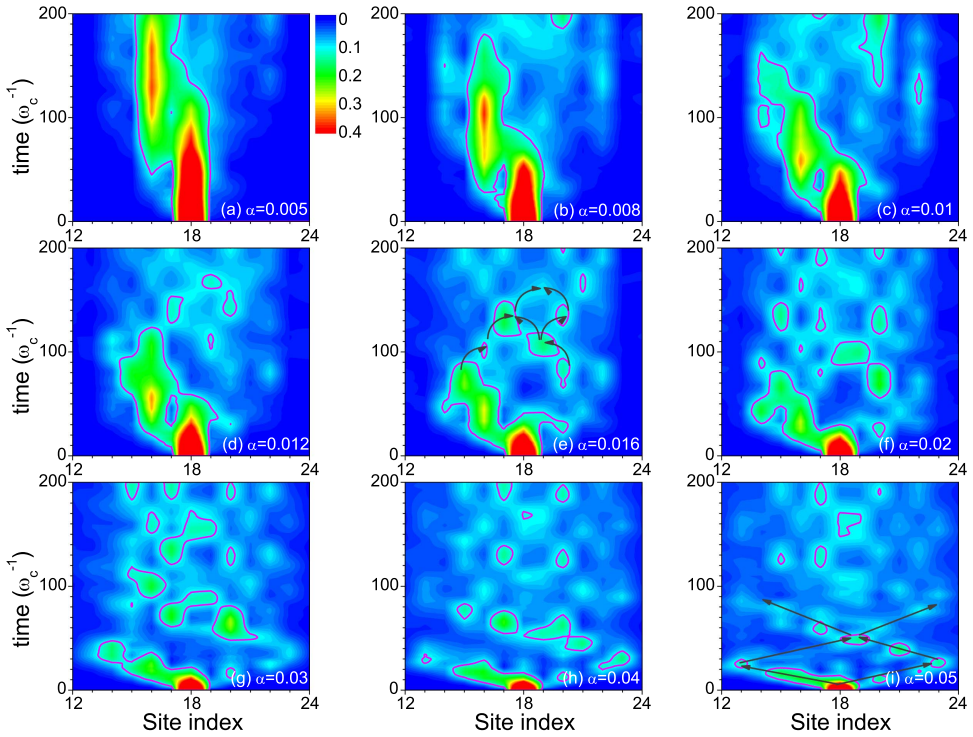

Figure 1. Evolution of electron population with nine α's from 0.005 to 0.05. The purple circles denote the populations larger than 0.1. The gray arrows in (e) and (i) denote the hopping directions.

3. Results and discussions

3.1. Dynamic localization

The evolution of the electron population is displayed in figure 1 for nine values of α, with the initial population located at site 18 (the original site). For $\alpha = 0.005$ and 0.008, the majority of the electron population is transferred to site 16 very quickly where the nearest local energy minimum related to the original site is located, implying a polaron is generated therein via the assistance of the e–p coupling, and over a long-term evolution the generated polaron is statically localized and immobile. For $\alpha > 0.01$, the situation changes. After a period of time the localized polaron starts to diffuse in a regime, which we follow Troisi *et al* in naming the dynamic localization regime [15, 18]. Taking $\alpha = 0.016$, for instance, when the time reaches around $100\omega_c^{-1}$ some bright spots emerge and are visibly separated, indicating the polaron is dynamically localized and the mechanism of the polaronic diffusion is similar to the hopping mechanism among the sites instead of the continuous wavefunction expansion, i.e. the band transport in a normal electronic lattice. Motivated by the wording 'band-like' and 'band', we hereafter name the new mechanism a 'hopping-like' mechanism to distinguish it from the well-known incoherent hopping mechanism. Following the time lapses, the diffused polarons reach the boundary of the dynamic localization regime and turn around and, as indicated by the arrows in figure 1(e), move towards its right hand side via hopping-like processes. The length of the dynamic localization regime, which is determined merely by the off-diagonal coupling, stands for the dynamic localization length [15]. We can find that, the stronger the off-diagonal coupling, the longer the dynamic localization length. In addition, as the system evolves over time, more bright spots appear in the dynamic localization regime, indicating that the polaron has access to more sites. For $\alpha \geqslant 0.03$, the hopping-like mechanism becomes even clearer, as indicated by the gray arrows in figure 1(i).

To show the polaron diffusion more clearly, the electron populations at $t < 50\omega_c^{-1}$ for $\alpha = 0.05$ are displayed in figure 2, where snapshots are taken for every $5\omega_c^{-1}$. It is found that the initial single peak of the electron wavepacket residing at the center of the chain splits into two that move individually to each side at $t < 25\omega_c^{-1}$. In the snapshot of $t = 25\omega_c^{-1}$, one can find two prominent peaks on site 13 and 23, implying that the polaron has moved 5 sites during the period. If the inter-site distance is a, the speed of the hopping-like transport is thus $0.2a\omega_c$. The speed depends on the e–p coupling so that the diffusion is α-dependent. At $t > 25\omega_c^{-1}$, the two peaks gradually rebound and merge together, implying that sites 12 and 24 serve as the boundaries of the dynamic localization regime for $\alpha = 0.05$. At $t = 40\omega_c^{-1}$, a single peak formed by the oppositely-heading peaks emerges at site 21, another site with energy minimum other than site 16. The process repeats in the subsequent evolution, as that shown in figure 1(i).

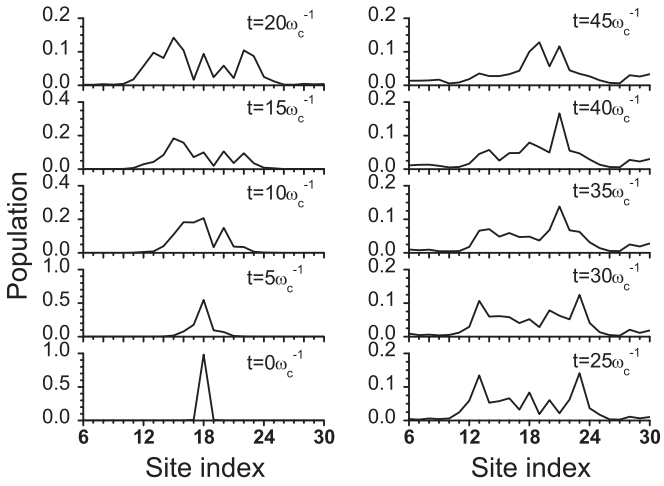

Figure 2. Electron populations at ten time points before $50\omega_c^{-1}$ for $\alpha = 0.05$.

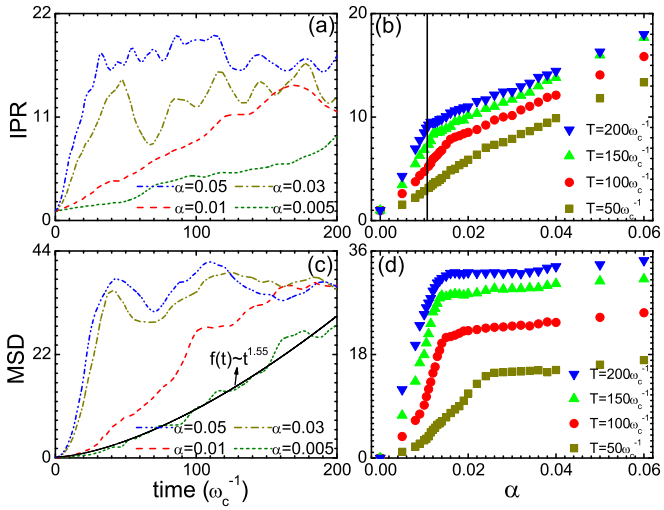

Figure 3. (a) Evolution of IPR for four values of α. (b) Temporal average value of IPR for four T's versus α. The black solid line denotes the transit point of the IPR-α slope. (c) Evolution of MSD for four values of α. The black solid curve denotes the fitting function $f(t) \sim t^{1.55}$ characterizing the super-diffusion. (d) Temporal average value of MSD for four T's versus α.

3.2. Quantum diffusion

In order to comprehend the transition of static and dynamic localization as well as the hopping-like mechanism, three quantities are calculated on the basis of the electron dynamics. The first one is the inverse participation ratio (IPR) defined by

$$R = \frac{1}{\sum_i \rho_i^2}, \tag{3}$$

where ρ_i is the electron population at site i. IPR is a well-defined measure of the localization length of electron wavefunction. The evolution of IPR is shown in figure 3(a) for four values of α. When $\alpha = 0.005$, IPR keeps increasing slowly until $t = 200\omega_c^{-1}$, implying the polaron extremely slowly broadens to the boundary of the localization regime. On the other hand, when $\alpha > 0.01$ the IPR quickly increases to a saturated value and then oscillates around it. The randomness of the oscillation comes from the energy disorder of the lattice chain. In order to gain an insight into the physical meaning of the results we calculate the temporal average via

$$\bar{R} = \frac{1}{T}\int_0^T R \cdot dt. \tag{4}$$

The average IPR is displayed in figure 3(b) for four T's. When $T = 50\omega_c^{-1}$ the average IPR exhibits an approximately linear relationship with α. On the other hand, when $T > 100\omega_c^{-1}$ a turnover emerges at around $\alpha = 0.0104$, as indicated by the black solid line in figure 3(b). This sudden change of the IPR-α slope tells us that

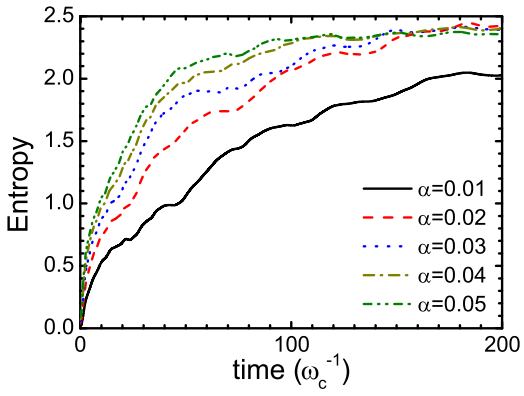

Figure 4. Evolution of entropy for five values of α.

there is a transition of the polaronic feature from static to dynamic localization. This is equivalent to the phase transition from insulator to poor metal discussed in [20, 21], as in the static localization regime the polarons are immobile while in the dynamic localization regime the polarons can move via the quantum diffusion (hopping-like mechanism). The finding is also compatible with the delocalization perspective of charge generation processes in organic solar cells, as addressed below.

The second quantity we calculate is the MSD, defined as

$$D = \sum_i (i - i_0)^2 \rho_i, \tag{5}$$

where i_0 is the original site. As discussed above, in the absence of an electric field the polaron exhibits super-diffusion, with $D \sim t^{1.55}$ [23]. Here, we fit the curve of $\alpha = 0.005$ with the function $f(t) \sim t^{1.55}$ and the tendency of the two is found to be in a good agreement, indicating that the very weak coupling case is close to the zero-field one. For large α, the MSD firstly increases and then saturates, sharing a similar tendency with that of IPR. Again, we calculate the temporal average of MSD as shown in figure 3(d). The relationship of MSD and T is similar to that of IPR and T. More interestingly, for large α the MSD becomes insensitive to α, quite different than in the case of IPR. This means for strong coupling the polaron becomes 'larger' than it does for weak coupling, while the localization length does not obviously depend on coupling in the phase of dynamic localization. As one could confuse the 'larger' polaron with the electron delocalization, this finding is significant for clarifying the intrinsic picture of charge generation in organics.

So far, one might wonder how the present scenario of polaronic quantum diffusion differs from the classical incoherent hopping mechanism. In other words, is the polaronic diffusion coherent or incoherent? We thus show the evolution of von Neumann entropy for the electron in figure 4. The von Neumann entropy is defined as

$$S = -\mathrm{Tr}\,\rho \ln \rho, \tag{6}$$

where ρ is the reduced density matrix of the electron system. Notably, the entropy is found to increase quickly in the beginning stage of the evolution when the polarons for the first time diffuse to the boundaries of the dynamic localization regime, and then saturates after $t > 100\omega_c^{-1}$ for $\alpha = 0.05$. For smaller α, it takes a longer time for the entropy to reach saturation. In $t < 200\omega_c^{-1}$, the saturated entropies for $\alpha \geqslant 0.02$ converge , and the entropy for $\alpha = 0.01$ keeps increasing. The entropy persists in the saturated value over a long-term evolution, showing that quantum coherence is not lost during polaronic diffusion, otherwise the entropy should decrease significantly since the polaron should incoherently localize in the individual site like the initial situation. As a result, the hopping-like mechanism recognized here is proven to be coherent. Different from incoherent hopping, it is not assisted by thermal fluctuation but promoted by the off-diagonal e–p interaction that accounts for the major driving force of ultrafast long-range charge separation in organic solar cells [11].

3.3. Random on-site energy

Lastly, we will further discuss the influence of the specific type of disorder. It is rational to expect that the deterministic Fibonacci lattice plays the same role as the disorder in the real materials. In figure 5, we show the population evolution in a lattice with completely random on-site energy for $\alpha = 0.05$. The on-site energy here is set to be a random number that is uniformly distributed between $-\epsilon_0$ and ϵ_0, and the results are averaged over five samples. Compared to figure 1(i), one can see that there are some quantitative differences between the two results, while the basic hopping-like process is present in both cases.

The type of disorder considered in this work is quite different from that in the Gaussian disorder model [12]. The latter is normally applied to amorphous organic semiconductors, in which the charge transport is more

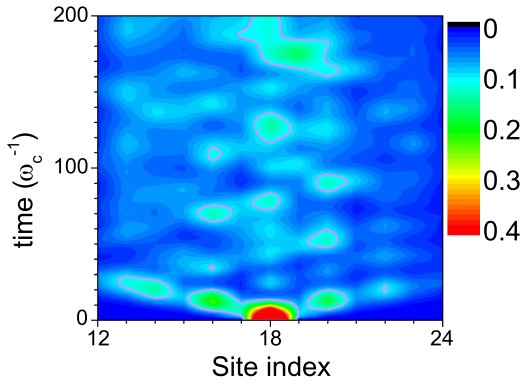

Figure 5. Evolution of electron population with $\alpha = 0.05$ for the lattice with random on-site energy. The purple circles denote the populations larger than 0.1.

likely to be normal diffusion. However, the experiment on the charge transport in doped polymers shows a power-law relationship for the electric current and temperature, indicating a super-diffusion transport [31]. This is why we have to go beyond the Gaussian disorder model to examine the super-diffusion behavior.

4. Conclusion and outlook

In summary, we have investigated the polaron dynamics in a Fibonacci lattice with respect to the off-diagonal e–p couplings. Two regimes, static and dynamic localization, are found for weak and strong e–p coupling, respectively. The polaron diffuses quantum mechanically in the dynamic localization regime, providing a novel scenario of a hopping-like mechanism for charge generation in organic solar cells.

As an outlook, we discuss more the applicability of the present dynamic localization scenario. In organic materials, charge photogeneration is understood to originate from the wavefunction delocalization [6, 7], since the electron-spin resonance experiment showed that the wavefunction of an electron is expanded to an extent of around 10 molecules [37]. Let us now alternatively analyze the current dynamic localization scenario. In common cases, the typical degree of site-energy disorder is 1 to $5k_{\mathrm{BT}}$, namely 0.026 to 0.12 eV at room temperature [32]. Let the characteristic disorder be 0.1 eV, i.e. $\epsilon_0 = 0.1$ in our model. The turnover value of α from static to dynamic localization as we found is 0.01. Since the typical energy of the intermolecular vibration mode is 7 meV, the coupling is then about 25 meV, which is a reasonable coupling strength in organic materials [33–36]. On the other hand, when the coupling is stronger than 25 meV, it is inferred from our findings that in organic solar cells, which consist of disordered molecular materials with moderate nonlocal e–p couplings, the charge generation can be elucidated by the mechanism of dynamic localization. The localization length would be about 10 times that of the intermolecular distance, which has been measured by the experiment [37]. Last but not least, this dynamic localization scenario is compatible with the conventional picture of delocalization [7] in the sense that the wavefunction of the electron does not localize in a single molecule. The difference between them is, however, that the dynamic localization mechanism survives the relatively strong disorder and gives a suitable e–p coupling, while delocalization does not.

Acknowledgments

The author gratefully acknowledges support from the National Natural Science Foundation of China (Grant Nos. 91333202 and 11574052). We thank W Yang and X Zhang for proofreading the manuscript.

References

[1] Evers F and Mirlin A D 2008 *Rev. Mod. Phys.* **80** 1355
[2] Anderson P W 1958 *Phys. Rev.* **109** 1492
[3] Coropceanu V, Cornil J, da Silva Filho D A, Olivier Y, Silbey R and Brédas J-L 2007 *Chem. Rev.* **107** 926
[4] Kilina S, Kilin D and Tretiak S 2015 *Chem. Rev.* **115** 5929
[5] Clarke T M and Durrant J R 2010 *Chem. Rev.* **110** 6736
[6] Bakulin A A, Rao A, Pavelyev V G, van Loosdrecht P H M, Pshenichnikov M S, Niedzialek D, Cornil J, Beljonne D and Friend R H 2012 *Science* **335** 1340
[7] Smith S L and Chin A W 2014 *Phys. Chem. Chem. Phys.* **16** 20305
[8] Falke S M *et al* 2014 *Science* **344** 1001

[9] Smith S L and Chin A W 2015 *Phys. Rev.* B **91** 201302(R)
[10] Bera S, Gheeraert N, Fratini S, Ciuchi S and Florens S 2015 *Phys. Rev.* B **91** 041107(R)
[11] Yao Y, Xie X and Ma H 2016 *J. Phys. Chem. Lett.* **7** 4830
[12] Bässler H 1993 *Phys. Status. Sol. (b)* **175** 15
[13] Yarkony D R and Silbey R 1977 *J. Chem. Phys.* **67** 5818
[14] Troisi A and Orlandi G 2006 *Phys. Rev. Lett.* **96** 086601
[15] Troisi A 2010 *Phys. Rev.* B **82** 245202
[16] Troisi A and Cheung D L 2009 *J. Chem. Phys.* **131** 014703
Fratini S and Ciuchi S 2009 *Phys. Rev. Lett.* **103** 266601
Ciuchi S, Fratini S and Mayou D 2011 *Phys. Rev.* B **83** 081202(R)
Wang L, Li Q, Shuai Z, Chen L and Shi Q 2010 *Phys. Chem. Chem. Phys.* **12** 3309
[17] Yao Y, Si W, Hou X and Wu C Q 2012 *J. Chem. Phys.* **136** 234106
[18] Wang T and Chan W-L 2014 *J. Phys. Chem. Lett.* **5** 1812
[19] Picon J-D, Bussac M N and Zuppiroli L 2007 *Phys. Rev.* B **75** 235106
[20] Di Sante D and Ciuchi S 2014 *Phys. Rev.* B **90** 075111
[21] Di Sante D, Fratini S, Dobrosavljević V and Ciuchi S 2017 *Phys. Rev. Lett.* **118** 036602
[22] Nazareno H N, de Brito P E and da Silva C A A 1995 *Phys. Rev.* B **51** 864
[23] de Brito P E, da Silva C A A and Nazareno H N 1995 *Phys. Rev.* B **51** 6096
[24] White S R 2004 *Phys. Rev. Lett.* **93** 076401
[25] Chin A W, Rivas Á, Huelga S F and Plenio M B 2010 *J. Math. Phys.* **51** 092109
[26] Prior J, Chin A W, Huelga S F and Plenio M B 2010 *Phys. Rev. Lett.* **105** 050404
[27] Guo C, Weichselbaum A, Kehrein S, Xiang T and von Delft J 2009 *Phys. Rev.* B **79** 115137
[28] Yao Y, Duan L, Lü Z, Wu C Q and Zhao Y 2013 *Phys. Rev.* E **88** 023303
[29] Yao Y 2015 *Phys. Rev.* B **91** 045421
Yao Y 2016 *Phys. Rev.* B **93** 115426
[30] Zhao Y, Yao Y, Chernyak V and Zhao Y 2014 *J. Chem. Phys.* **140** 161105
Yao Y, Zhou N, Prior J and Zhao Y 2015 *Sci. Rep.* **5** 14555
[31] Kronemeijer A J, Huisman E H, Katsouras I, van Hal P A, Geuns T C T, Blom P W M, van der Molen S J and de Leeuw D M 2010 *Phys. Rev. Lett.* **105** 156604
[32] Coehoorn R, Pasveer W F, Bobbert P A and Michels M A J 2005 *Phys. Rev.* B **72** 155206
[33] Hatch R C, Huber D L and Höchst H 2010 *Phys. Rev. Lett.* **104** 047601
[34] Girlando A, Grisanti L and Masino M 2010 *Phys. Rev.* B **82** 035208
[35] Li Y, Yi Y, Coropceanu V and Brédas J-L 2012 *Phys. Rev.* B **85** 245201
[36] Li Y, Coropceanu V and Brédas J-L 2013 *J. Chem. Phys.* **138** 204713
[37] Marumoto K, Kuroda S, Takenobu T and Iwasa Y 2006 *Phys. Rev. Lett.* **97** 256603